An Online Eccentricity Fault Detection Method for Axial Flux Machines

Seyyed Mehdi Mirimani[1], Abolfazl Vahedi[1], Fabrizio Marignetti[2], *Senior member, IEEE,* and Roberto Di Stefano[2]

[1] Center of Excellence for Power Systems Automation and Operation, Dept. of Electrical Engineering of Iran University of Science & Technology , Tehran, Iran
[2] Department of Electrical and Information Engineering, University of Cassino and Southern Latium, Italy

***Abstract* -- An eccentric air-gap creates an electromagnetic force between the rotor and the stator of electrical machines. This force is known as unbalanced magnetic pull (UMP). This force leads to further increase the eccentricity and may severely reduce the performance of the machine, producing acoustic noise, vibration, excessive wear of bearing, rotor and stator rubbing. This paper presents a universal online method for diagnosing eccentricity in Axial Flux Permanent Magnet (AFPM) Machine. It is based on measuring the induced voltages of three search coils positioned above the coils of three phases as a suitable criterion for fault detection. Using this number of search coils enables not only the Static Eccentricity Factor (SEF) but also the minimum air-gap position to be estimated. The Three-Dimensional Finite-element Method (3D-FEM) was used to accurately analyze the machine and to validate the method. This study indicates that the induced voltages of the search coils suggest an online method for indirectly measuring eccentricity during machine operation.**

***Index Terms*-- Axial flux permanent magnet machine, fault diagnosis, three-dimensional finite-element method (3D-FEM).**

I. INTRODUCTION

The existence and the effects of eccentricity in electrical machines have been investigated for more than 100 years [1]. An eccentric rotor motion happens when the rotation axis of an electrical machine does not overlap with the axis of the stator bore. Due to built-in tolerances, wear of bearings, and other reasons, some degree of rotor eccentricity is always present. Rotor eccentricity produces the electromagnetic force which is known as unbalanced magnetic pull (UMP) acting between the rotor and the stator [2]. It is therefore very important to achieve an estimate of eccentricity for diagnosis and monitoring purposes. This study deals with this issue.

There has been a growing interest in AFPM machines over the last decade and they are being increasingly used in various applications due to their high-efficiency, compact construction and high torque at low speeds. AFPMs are being used in several applications such as low-speed turbines, distributed generation (DG), electric vehicles (EV) and traction [3]–[7]. One important issue is to detect the electrical and mechanical faults in these machines. Mechanical faults are common in electric machines, and represent up to 60% of the total faults [8]. Approximately, 80% of mechanical faults produce eccentricity [9]. Bearing faults and eccentricity are among the critical and severe mechanical faults [10]. In fact, electrical machines are subject to a number of defects during operation that reduce their lifetime. So it is very important to maximize the lifetime of machine by using appropriate fault detection methods. One challenge in this step is to define the appropriate criterion for fault detection.

Eccentricity fault detection in Radial Flux-Permanent Magnet Synchronous Machines (RF-PMSM) is well covered in the literature. However there would appear to be no research on diagnosing eccentricity in AFPMs, which indicates the novelty of the subject dealt with in this paper. Mirimani *et al.* have shown that air-gap eccentricity has significant effects on the air-gap flux and consequently results in UMF in AFPMs. Also UMF was shown to produce an undesirable magnetic torque that may cause bearing faults and motor condition deterioration. Furthermore, it was shown that eccentricity in AFPMs occurs even with low rotor deviations. This fact increases the rate of SE in AFPMs [11].

The proposed method of this study is based on measuring induced voltages in three search coils. Using search coils in order to find a good criterion for fault detection has been investigated in several studies. In [12] two search coils were located in the air-gap for detecting the presence of shorted rotor turns in synchronous machine and it was shown that the method was working well on no-load and low load conditions. Moreover, fault position could also be indicated by a simple detection system. Kim *et al.* have shown that eccentricity fault diagnosis using the current signal and vibration signal analysis are very difficult because of the switching harmonics of the drive system [13]. Therefore, the search coil was used for the eccentricity diagnosis of the motor. The back EMFs at the search coil were compared in both the normal and eccentric conditions and it was shown that the induced voltage of the search coil gave a good criterion for eccentricity fault detection. But the problem with this study is that there is a single search coil in the air-gap which makes the method sensitive to the minimum air gap position. Da *et al* also proposed a novel approach to health monitoring and multi fault detection in permanent magnet synchronous machines using direct flux measurement with search coils [14]. One benefit of this technique was that the load condition does not necessarily need to be specified for accurate fault diagnosis. Furthermore, the direction of eccentricity and the location of winding shorted turns could be found. Also, in

978-1-4799-4749-2/14/$31.00 ©2014 IEEE

[15] it was observed that eccentricity faults in AFPMs may be diagnosed by monitoring the harmonics in the stator coil induced voltage spectra at no-load condition. It was found that in an eccentric condition the unbalanced back EMF proposes a method for indirectly detect eccentricity which could be used during assembling and manufacturing processes or maintenance operations.

In this paper a novel online method is presented for diagnosing eccentricity in AFPMs. The proposed method is based on measuring induced voltages in three search coils located in slots of three different phases. It is also shown that the method does not depend on load condition.

II. Static Eccentricity In AFPMs

Eccentricity is the misalignment of the stator and rotor axes and the rotational axis of the rotor. As shown in Fig. 1, an unbalanced air-gap appears in AFPMs when the rotor is axially inclined. If the rotor shaft assembly is adequately rigid, the level of eccentricity remains constant. In this case, the air-gap is not uniform throughout the rotor circumference but is time-independent. In other words, in the case of static eccentricity the position of the minimum air-gap length is fixed in space. As discussed in [11], SEF can be defined as follows:

$$SEF = \frac{r}{g_0} \times 100\% \quad (1)$$

Where g_0 is the air-gap length in healthy condition and r is the air-gap variation at the position of maximum or minimum air-gap length. Also, SEF can be written as a function of the angle of deviation:

$$SEF = \frac{R_{mid}.\sin(\beta)}{g_0} \times 100\% \quad (2)$$

Where R_{mid} is the mean radius that is mentioned at the middle of magnets illustrated in Fig. 1. As shown in [11] in order to reach to a high value of SEF, a high deviation angle is not needed, because of the high ratio of machine diameter to length in AFPMs. So, in the assembling process and also during motor operation, a non-uniform air-gap is very likely to exist.

III. Specifications of the Machine

The proposed fault diagnosis method is applied to a 3-phase 28-pole AFPM, as illustrated in Fig. 2. It consists of a stator with 24 slots and 12 single layer trapezoidal shaped coils with concentrated winding. Details of machine dimensions and nominal values are given in Table I. Also, the motor winding consists of four coils in each phase that are in series and the phase connection is delta. The rated speed of the motor is 1285 rpm and the nominal voltage is 210 V. Also, more details about the AFPM were investigated in [11], [15].

I. Finite Element Simulation

Modeling surface-mounted PMSMs can be performed via analytical, two-dimensional finite-element method (2D-FEM) or 3D-FEM.

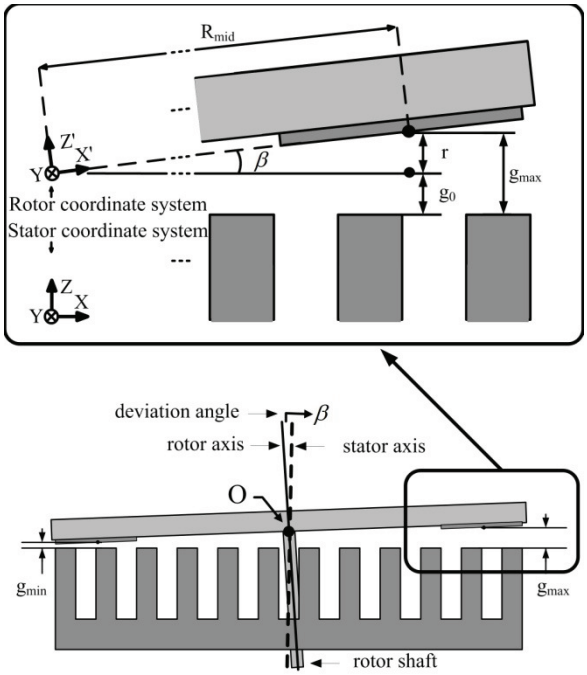

Fig. 1. Static Eccentricity in AFPMs.

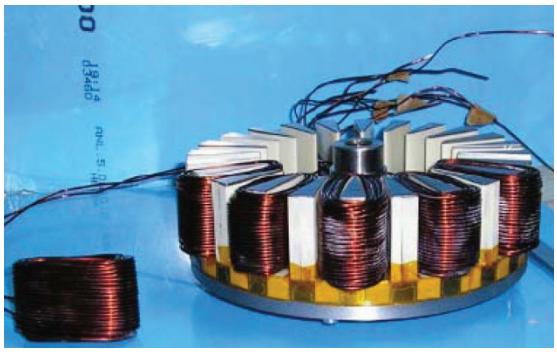

Fig. 2. Investigated AFPM.

TABLE I
AFPM Specifications

Quantity	Value	Quantity	Value
Rated power(kW)	2.2	Stator outer diameter (mm)	200
No-load voltage(V)	210	Stator inner diameter (mm)	116
Rated phase current(A)	3.5	Slot width(mm)	13.6
Frequency(Hz)	300	Slot height(mm)	40
Speed(rpm)	1285	Number of slots	24
Phase connection	Δ	Stator back iron width (mm)	10.5
Pole pairs	14	Rotor back iron width (mm)	10
Air gap length(mm)	1.5	Wire diameter(mm)	1.5
Rotor diameter(mm)	206	Number of turns per coil	130
Magnet remanence (T)	1.24	Phase resistance at 300Hz(Ω)	2.5
Magnet thickness (mm)	3	Stator inductance(mH)	10

In industrial purposes, the analytical approach or 2-D FEM is rather used in computations owing to their speed compared to the 3D-FEM. The magnetic path of an axial flux machine is not contained in a 2D plane. Thus, axial flux machines are inherently 3-D machines from the point of view of geometry modeling. Therefore, analytical and 2-D FEM analysis, usually carried out on the average radius of the machine, do not usually yield enough accuracy in computations. Regarding the purpose of this paper to diagnose the SE there is need for an accurate modeling that takes into account the saturation effects and all geometric

details such as stator and rotor slotting. Therefore, 3D-FEM was utilized in order to study SE fault detection in AFPMs. The simulations have been done by the software FLUX3D [17]. Fig.3 shows the 3-D FEM model of machine. The coils with the same color belong to one phase. The simulations are based on a circuit coupled model. Two layers of elements are in the air-gap to achieve precise results. The total number of nodes is 460,000 in this simulation. It should be noted that due to asymmetric air-gap, the geometry of machine is not periodic; therefore the entire geometry was modeled. The center of the stator is fixed at the origin of the global coordinate system and the center of the rotor is located at the origin of a local coordinate system. In order to generate eccentricity, the rotor coordinate system is deviated of β around *y*-axis and also the rotor rotates around the *z*-axis of its own coordinate system [see Fig. 1].

II. Proposed Fault Diagnosis Method

The proposed method is based on measuring the induced voltages of three search coils C_1, C_2 and C_3 placed at φ = 0°,120° and 240° [see Fig. 4]. In this figure, φ is the angle measured from a reference point on the stator. The coils are displaced by α =120° and therefore they are located above the coils of three different phases. Fig. 5 shows the induced voltages of three search coils with an air-gap length of 1.6 mm at speed of 675 rpm. These three search coils made of eighteen turns are modeled in 3D-FEM in order to calculate the induced voltages. The rms values are 3.5 V and they depend on the air-gap values and rotational speed. Fig. 6 shows the effect of speed and air-gap variations on the induced voltages of each coil. It can be seen that by increasing the speed and decreasing the air-gap length, the induced voltages are increased. The proposed method for diagnosing SE is able not only to estimate the SEF but also to define the position of the minimum air-gap. Firstly, it should be noted that the amplitude of the induced voltage of each search coil is proportional to the air-gap length above each coil. If the latter is reduced, the induced voltage amplitude is increased. If there is no eccentricity, the air-gap length is equal for each search coil and consequently the amplitudes of induced voltages will be equal. Along each axis, a vector is assumed with the amplitude of search coil voltage and orientation of the coil axis. In a healthy condition, the result of these vectors approaches zero, estimating SEF as zero. In an eccentric condition, the vectors close to the minimum air-gap become larger directing the resultant vector toward their own direction. Hence, the result of these three vectors has amplitude corresponding to SEF and a direction toward the minimum air-gap position. The outcome vector of $\overline{C_1}$, $\overline{C_2}$ and $\overline{C_3}$ can be written as follows:

$$\overline{C_{total}} = \overline{C_1} + \overline{C_2} + \overline{C_3} \tag{3}$$

The X component of the vector can be written as:

$$|\overline{C_{total,x}}| = |\overline{C_1}|.\cos(0°) + |\overline{C_2}|.\cos(120°) + |\overline{C_3}|.\cos(240°) \tag{4}$$

And also the Y component as:

$$|\overline{C_{total,y}}| = |\overline{C_1}|.\sin(0°) + |\overline{C_2}|.\sin(120°) + |\overline{C_3}|.\sin(240°) \tag{5}$$

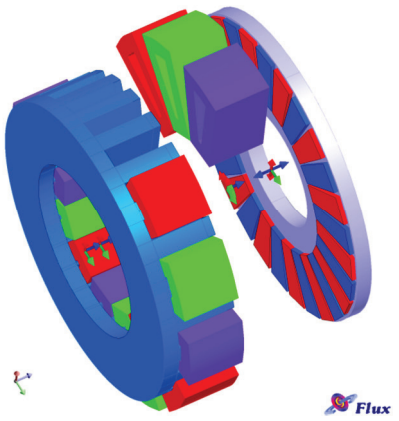

Fig. 3. 3-D FEM model of machine.

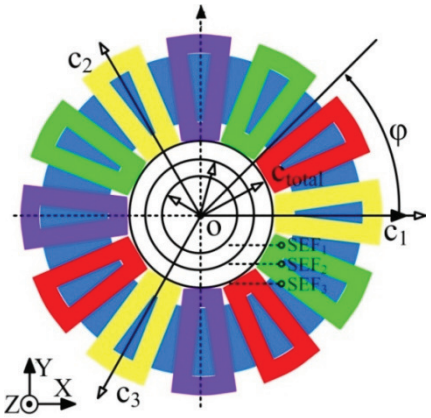

Fig. 4. Search coil locations. The search coils are mechanically spaced by 120° .

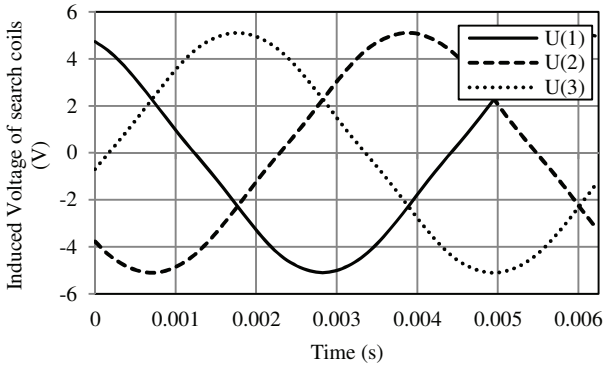

Fig.5 Induced voltages of three search coils at a speed of 675 rpm calculated by FEM analysis (the rms values are 3.5 V).

The matrix form is:

$$[|\overline{C_{total,x}}| \quad |\overline{C_{total,y}}|] = [|\overline{C_1}| \; |\overline{C_2}| \; |\overline{C_3}|].\begin{bmatrix} 1 & 0 \\ -0.5 & \sqrt{3}/2 \\ -0.5 & -\sqrt{3}/2 \end{bmatrix} \tag{6}$$

The SEF can be estimated by the amplitude of $|\overline{C_{total}}|$:

$$SEF \approx |\overline{C_{total}}| = \sqrt{|\overline{C_{total,x}}|^2 + |\overline{C_{total,y}}|^2} \tag{7}$$

And the minimum air-gap position can be estimated as:

$$\theta = \arctan(|\overline{C_{total,y}}|/|\overline{C_{total,x}}|) \tag{8}$$

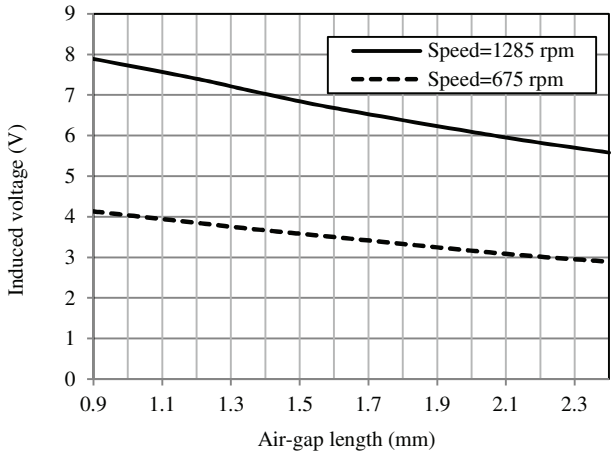

Fig.7 Search coils induced voltages variations versus air-gap length calculated by FEM analysis.

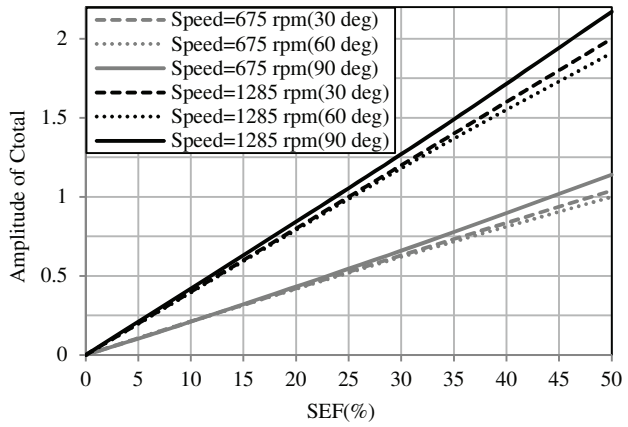

Fig.8 Value of $|\overline{C_{total}}|$ versus SEF for different speeds calculated by FEM analysis. This curve will be used for estimating SEF.

TABLE II
Scenarios relating to states with different degrees of eccentricity and minimum air-gap position of 30 degree

Speed=675 rpm						
Imported SEF	$\lvert\overline{C_1}\rvert$	$\lvert\overline{C_2}\rvert$	$\lvert\overline{C_3}\rvert$	$\lvert\overline{C_{total}}\rvert$	Estimated θ	Estimated SEF (%)
0	3.50	3.51	3.51	0.008	-	-
10	3.62	3.52	3.37	0.21	34	10.0
30	3.86	3.56	3.13	0.63	35	30.1
50	4.14	3.6	2.9	1.04	33	49.7
Speed=1285 rpm						
Imported SEF	$\lvert\overline{C_1}\rvert$	$\lvert\overline{C_2}\rvert$	$\lvert\overline{C_3}\rvert$	$\lvert\overline{C_{total}}\rvert$	Estimated θ	Estimated SEF (%)
0	6.67	6.68	6.68	0.009	-	-
10	6.89	6.72	6.44	0.39	38	9.8
30	7.36	6.8	6	1.2	36	30.1
50	7.9	6.9	5.6	2	34	50.2

III. ESTIMATING METHOD

In order to validate the proposed diagnosis method, different eccentricity degrees of 10%, 30% and 50% are considered with one random minimum air-gap positions placed at φ = 30°. Rms values of induced voltages on coils $|\overline{C_1}|$, $|\overline{C_2}|$ and $|\overline{C_3}|$ are obtained in 8 scenarios that are shown in Table II. Then the $|\overline{C_{total}}|$ versus SEF was calculated using FEM analysis for two speeds, namely 675 rpm and the nominal one of 1285 rpm. The results are shown in Fig. 8 and can be used to estimate the value of SEF under faulty condition. It should be noted that the relation depends on both values of SEF and speed. It can be seen that the value of $|\overline{C_{total}}|$ is increased by increasing SEF. This happens because in an eccentric condition the values of $|\overline{C_1}|$, $|\overline{C_2}|$ and $|\overline{C_3}|$ are not balanced. Therefore, the value of the outcome vector will be larger and each value of SEF is corresponding to a special value of $|\overline{C_{total}}|$ which can be used in fault detection purpose. As shown in Fig. 8, the values are calculated for different minimum air-gap positions which show approximately the same manner. It can be noted that for higher eccentricities error of lower than 5% in estimating SEF is achieved which is acceptable for diagnostic purposes. Each value of $|\overline{C_{total}}|$ is therefore related to an SEF. Also in estimating air-gap position using equation (8), as observed in Table II, the maximum error of 8 degrees is obtained which is acceptable. In fact, it can be stated that the accuracy of the presented method in estimating the minimum air-gap position is greater than the slot pitch of the machine which is 15 degrees.

To summarize, one point of Fig. 8 should be calculated for any machine at one speed, then all other lines are achievable as the induced voltages are proportional to rotational speed. Regarding to these facts it can be concluded that the $|\overline{C_{total}}|$ can be written as follows:

$$|\overline{C_{total}}| = K_m . \omega . SEF \quad (9)$$

Where K_m is a coefficient obtained from one point of Fig. 8 and ω is the rotational speed. This equation describes the Fig. 8 in an analytical approach. Equation (9) shows that there is a unique relation between $|\overline{C_{total}}|$ and SEF which makes the diagnosis process applicable.

To summarize, for industrial purposes the K_m should be calculated for any machine, thereby allowing the value of SEF to be easily estimated at any speed for the AFPM considered. In the case of investigated machine the K_m is 0.000031. The estimated values of SEF in Table II are calculated using equation (9) that shows a very good agreement with the imported SEF in FEM simulation.

IV. CONCLUSION

A novel method for diagnosing eccentricity in AFPM machines was presented in this paper. It is based on measuring induced voltages in three search coils located above the main coils of three different phases.

3D-FEM was used to yield enough accuracy in computations of the induced voltages with a transient electromagnetic solver. Using FEM the proposed model was validated and it was shown that there is a linear relation between proposed criterion and SEF that has eased the fault detection process.

It was observed that use of this method made it possible not only the SEF to be estimated but also the minimum air-gap position with a good precision.

V. REFERENCES

[1] J. Fisher-Hinnen*, Dynamo Design*. New York: Van Nostrand, 1899.

[2] A. Burakov and A. Arkkio, "Comparison of the unbalanced magnetic pull mitigation by the parallel paths in the stator and rotor windings ," *IEEE Trans. Magn.*, vol. 43, no. 12, pp. 4083–4088, Dec. 2007.

[3] R. Di Stefano, F. Marignetti, "Electromagnetic Analysis of Axial-Flux Permanent Magnet Synchronous Machines With Fractional Windings With Experimental Validation," *IEEE Trans. Ind. Electron.*, vol. 59, no. 6, pp. 2573-2582, Jun. 2012.

[4] G. De Donato, F. G. Capponi, F. Caricchi, "No-Load Performance of Axial Flux Permanent Magnet Machines Mounting Magnetic Wedges," *IEEE Trans. Ind. Electron.*, vol. 59, no. 10, pp. 3768-3779, Oct. 2012.

[5] G. De Donato, F. G. Capponi, F. Caricchi, "On the Use of Magnetic Wedges in Axial Flux Permanent Magnet Machines ," *IEEE Trans. Ind. Electron.*, vol. 60, no. 11, pp. 4831–4840, Nov. 2013.

[6] H. Vansompel, P. Sergeant, and L. Dupré, "Optimized design considering the mass influence of an axial flux permanent-magnet synchronous generator with concentrated pole windings," *IEEE Trans. Magn.*, vol. 46, no. 12, pp. 4101–4107, Dec. 2010.

[7] N. P. Shah, A. D. Hirzel, Cho. Baekhyun, "Transmissionless Selectively Aligned Surface-Permanent-Magnet BLDC Motor in Hybrid Electric Vehicles," *IEEE Trans. Ind. Electron.*, vol. 57, no. 2, pp. 669-677, Feb. 2010.

[8] J. Faiz, B. M. Ebrahimi, B. Akin, and H. A. Toliyat, "Comprehensive eccentricity fault diagnosis in induction motors using finite element method," *IEEE Trans. Magn.*, vol. 45, no. 3, pp. 1764–1767, Mar. 2009.

[9] J. Faiz, B. M. Ebrahimi, and H. A. Toliyat, "Effect of magnetic saturation on static and mixed eccentricity fault diagnosis in induction motor," *IEEE Trans. Magn.*, vol. 45, no. 8, pp. 3137–3144, Aug. 2009.

[10] J. Faiz, B. M. Ebrahimi, B. Akin, and H. A. Toliyat, "Comprehensive eccentricity fault diagnosis in induction motors using finite element method," *IEEE Trans. Magn.*, vol. 45, no. 3, pp. 1764–1767, Mar. 2009.

[11] S. M. Mirimani, A. Vahedi, and F. Marignetti, "Effect of inclined static eccentricity fault in single stator–single rotor axial flux permanent magnet machines," *IEEE Trans. Magn.*, vol. 48, no. 1, pp. 143–149, Jan. 2012.

[12] R.L. Stoll and A. Hennache, "Method of detecting and modelling presence of shorted turns in DC field winding of cylindrical rotor synchronous machines using two airgap search coils," *IET Elect. Power Appl.*, vol. 135, no. 6, pp. 281–294, Nov. 1988.

[13] M. J. Kim, B. K. Kim, J. W. Moon, Y. H. Cho , D. H. Hwang and D. S. Kang, "Analysis of inverter-fed squirrel-cage induction motor during eccentric rotor motion using FEM," *IEEE Trans. Magn.*, vol. 44, no. 6, pp. 1538–1541, Jun. 2008.

[14] Y. Da, X. Shi, C. Kral, and M. Krishnamurthy, "A new approach to fault diagnostics for permanent magnet synchronous machines using electromagnetic signature analysis," *IEEE Trans. Power Electron.*, vol. 28, no. 8, pp. 4104–4112, Aug 2013.

[15] S. M. Mirimani, A. Vahedi, F. Marignetti and E.D.Santis, "Static Eccentricity Fault Detection in Single Stator-Single Rotor Axial Flux Permanent Magnet Machines," *IEEE Trans. Ind. Appl*, vol. 48, no. 6, pp. 1838–1845, Nov./Dec. 2012.

[16] A. Parviainen, M. Niemelä, and J. Pyrhönen, "Modeling of Axial Flux Permanent-Magnet Machines," *IEEE Trans. Magn.*, vol. 40, no. 5, pp. 1333–1340, Sep./Oct. 2004.

[17] *Flux3D User's Guide*, ver. 10.3.3, CEDRAT Group, Meylan, France, 2011.